Version of Record: https://www.sciencedirect.com/science/article/pii/S0045782523004632
Manuscript_0289cf55f63821501c1f3c4cb0bc6df0

Stochastic Modeling and Statistical Calibration with Model Error and Scarce Data

Zhiheng Wang[a,*], Roger Ghanem[a]

[a]*Sonny Astani Department of Civil and Environmental Engineering, University of Southern California, 210 KAP Hall, Los Angeles, CA 90089, USA*

Abstract

This paper introduces a procedure to assess the predictive accuracy of stochastic models subject to model error and sparse data. Model error is introduced as uncertainty on the coefficients of appropriate polynomial chaos expansions (PCE). The error associated with finite sample size allows us to conceive of these coefficients as statistics of the data that we describe as random variables whose influence on output quantities of interest is evaluated through the extended polynomial chaos expansion (EPCE). A Bayesian data assimilation scheme is introduced to update these expansions by considering the resulting nested chaos expansion as a hierarchical probabilistic model. Stochastic models of quantities of interest (QoI) are thus constructed and efficiently evaluated. The Metropolis-Hastings Markov chain Monte Carlo procedure is used to sample the posterior. Two illustrative analytical and numerical problems are used to demonstrate the proposed approach.

Keywords: Model error, Scarce data, Bayesian inference, Extended polynomial chaos expansion, Polynomial chaos coefficients, Uncertainty quantification.

1. Introduction

Uncertainties exist in many areas of science and engineering, and the manner of dealing with them for purposes of prediction continues to be of widespread interest [1, 2, 3, 4] . All physics models, including experimental devices and computational codes, provide mere approximations of their intended behavior. The input parameters (e.g. material properties, load characteristics) of a physics model can have intrinsic and irreducible randomness which is often referred to as "aleatoric uncertainty" [1] . These uncertain input parameters are typically modeled as random variables whose probability distributions are inferred from availale data. As they are propagated through a sequence of physics models, the input uncertainties are transformed into uncertainties on quantities of interest (QoI) relevant to design and decision-making [5]. Subsequent observations of these QoI or other functional of the physical behavior of the system can conceptually be used to update prior belief concerning aleatoric variables [6]. Two observations are relevant in this context and for defining the scope of this paper. First, any mathematical model is at best an approximation of an intended physical phenomenon. Errors in the physics model introduce bias in comparing model predictions to observations. Second, estimating prior probabilistic models from limited data introduces statistical errors in these models [7]. These errors in the probabilistic model motivate the idea of propagating forward a family of priors that capture the statistical error introduced by the finite sample size. These forms of model error can be referred to as "epistemic" and are reducible by acquiring, respectively, additional physics insight or more experimental data.

The physics model error (often referred to as model inadequacy) refers to the discrepancy between prediction and reality and can result from the effect of simplifications and mis-representations of the modeled

*Corresponding author.
Email address: zhihengw@usc.edu (Zhiheng Wang)

phenomenon. Thus, model error is inevitably random and is usually charcaterized through model validation [8, 9]. It is common to represent model error with a completely statistical formulation and calibrate it with observations. In view of their simplicity, and in spite of their lack of physical consistency, Gaussian representations for this model inadequacy [10] are widely adopted in many application domains. Recently, there has been a concerted effort at developing more physically meaningful model such as random matrix models [11], the stochastic inadequacy operator [12], and embedded model errors [13, 14]. These constructions attempt to varying degrees, to satisfy known physics constraints.

Surrogate models (also known as metamodels) have gained increasing popularity for model validation and calibration in the past few decades, particularly in complex engineering and scientific applications [15, 16, 17, 18, 19, 20, 21] . Such models are typically trained on input output pairs from the physics model, yielding a black box that can mimic significant traits of the underlying full fidelity model. Challenges to this paradigm pertain to the achievable tolerances in reproducing specific traits of the underlying system and to the requisite size of the training set.

A typical manner to deal with epistemic uncertainty associated with incomplete probability information has been to perform nested iterations, with aleatory analysis on the inner loop and epistemic analysis on the outer loop [22, 23]. In this case, the two types of uncertainties can be separated and easily traced. In particular, each realization of the probabilistic models generates a response PDF based only on the basic random variables. Thus, the ensemble of response PDFs evaluated at a number of realizations of the probabilistic models can be used to visualize the combined uncertainty in the response and further interpret the results using various statistical metrics. This paradigm, while conceptually simple, is computationally prohibitive. Many researches have been focusing on modeling and propagating the uncertainty model for the input parameters with sparse data, including evidence theory [24, 25], fuzzy set theory [26, 27] and interval analysis [28].

The polynomial chaos expansion (PCE) formalism is not a standard surrogate model. Specifically, PCE first embeds the physics model at hand in a larger family of models. This family is parameterized by white noise, a collection of independent variables, which simultaneously shapes both input and output. While this embedding brings about the curse of dimensionality, it also provides a comprehensive mathematical structure that serves to address the issues of convergence and efficiency raised above [29, 30, 31, 32]. The independent variables at the core of the PCE are often referred to as the stochastic germ or the stochastic degrees of freedom. These germs attempt to capture the independent statistical pieces of information needed to characterize the quantities of interest, which often include (but not limited to) information required to characterize the physics. In the standard PCE, this germ is associated with the prior model of the input parameters. A statistically coherent perspective conceived the PCE model as a statistical model, and estimated its parameters using either likelihood [33, 34, 35] or Bayesian [36] arguments. The Extended PCE (EPCE) [37, 38, 39, 40, 41] formalized this "bookkeeping" of uncertainty by extending the germ to include, as part of the model structure, stochastic degrees of freedom that tag information about the prior probabilistic model. The present papers presents one Bayesian formalism that leverages the EPCE construction, while also providing context for the uncertainty in the physics model.

The paper is structured as follows. In Sections 2 and 3, we provide detailed overview of PCE and EPCE surrogate models, respectively. Then, in Section 4, we introduce the construction of PCE with random coefficients in which the uncertainty reflects the error associated with incomplete data. Following that, we describe the procedure of updating the random PCE coefficients built in Section 5 using MCMC, as well as a brief overview of the standard Bayesian approach to infer the physical model parameters implemented with additive Gaussian model error. Then stochastic models of QoI are introduced for validation metrics in Section 6. Finally, the proposed procedure is illustrated by one analytical and one numerical example in Section 7 and we present the conclusions and some closing comments in Section 8.

2. Review: Polynomial Chaos Expansion

Let X represent a scalar QoI that can be expressed as a function of a vector $\boldsymbol{K} = \{K_1, \cdots, K_d\}$ representing physical random parameters such that $X = g(\boldsymbol{K})$. The d-dimensional vector $\boldsymbol{K}$ is first expressed as a mapping from a d-dimensional vector $\boldsymbol{\xi} = \{\xi_1, \cdots, \xi_d\}$ of uncorrelated standard normal random variables

using, for instance, the Rosenblatt transformation. The set $\boldsymbol{\xi}$ is referred to as the "germ" or the stochastic degrees of freedom of the uncertainty. Expressing X as a function of $\boldsymbol{\xi}$ and representing $X(\boldsymbol{\xi})$ in an orthogonal polynomial expansion with respect to $\boldsymbol{\xi}$ yields the polynomial chaos expansion (PCE) of X relative to $\boldsymbol{\xi}$,

$$X(\boldsymbol{\xi}) = \sum_{|\boldsymbol{\alpha}| \leq p} X_{\boldsymbol{\alpha}} \psi_{\boldsymbol{\alpha}}(\boldsymbol{\xi}), \qquad \boldsymbol{\xi} \in \mathbb{R}^d, \boldsymbol{\alpha} \in \mathbb{N}^d \tag{1}$$

where $\{X_{\boldsymbol{\alpha}}\}$ are referred to as the PCE coefficients, p denotes the highest order in the polynomial expansion, $\boldsymbol{\alpha}$ is a d-dimensional multi-index, and $\{\psi_{\boldsymbol{\alpha}}\}$ are the normalized multivariate Hermite polynomials that can be expressed in terms of their univariate counterparts as follows,

$$\psi_{\boldsymbol{\alpha}}(\boldsymbol{\xi}) = \prod_{p=1}^{d} \psi_{\alpha_p}(\xi_p) = \prod_{p=1}^{d} \frac{h_{\alpha_p}(\xi_p)}{\sqrt{\alpha_p!}} \ , \qquad \boldsymbol{\xi} \in \mathbb{R}^d, \boldsymbol{\alpha} \in \mathbb{N}^d \tag{2}$$

where, h_{α_p} represents the one-dimensional Hermite polynomial of order p. The collection of the multivariate polynomials forms an orthogonal set with respect to the multivariate Gaussian density function.

In order to emphasize its dependence on the PCE representation, we denote the realization of X synthesized from its PCE using sample $\boldsymbol{\xi}^{(i)}$ of $\boldsymbol{\xi}$ by,

$$X^{(i)} \triangleq X(\boldsymbol{\xi}^{(i)}, \{X_{\boldsymbol{\alpha}}\}) = \sum_{|\boldsymbol{\alpha}| \leq p} X_{\boldsymbol{\alpha}} \psi_{\boldsymbol{\alpha}}(\boldsymbol{\xi}^{(i)}). \tag{3}$$

The above PCE decomposition converges to $X(\boldsymbol{\xi})$ in mean-square and thus also in distribution. The PCE coefficients $X_{\boldsymbol{\alpha}}$ is the expectation of the product $X(\boldsymbol{\xi})\psi_{\boldsymbol{\alpha}}(\boldsymbol{\xi})$ and can thus be expressed as a d-dimensional integral to be estimated as a weighted sum of samples of $X(\boldsymbol{\xi})$. This can be achieved either using a sampling such as Monte Carlo or Quasi-Monte Carlo techniques or by relying on a quadrature approximation as follows,

$$X_{\boldsymbol{\alpha}} = \sum_{q \in Q} X(\boldsymbol{\xi}^q) \psi_{\boldsymbol{\alpha}}(\boldsymbol{\xi}^q) w_q, \quad |\boldsymbol{\alpha}| \leq p \ , \tag{4}$$

where, Q is a quadrature rule in $\mathbb{R}^d$, $\xi 1$ is a quadrature node in Q and w_q is the associated weight. The quadrature level required to achieve a preset accuracy in approximating any $X_{\boldsymbol{\alpha}}$ increases with the order of the associated polynomial, $\psi_{\boldsymbol{\alpha}}$. For a given polynomial order p and germ dimension d, the number of these PCE coefficients, denoted by N_{pce}, is equal to,

$$N_{\text{pce}} = \frac{(d+p)!}{d!\ p!}. \tag{5}$$

3. Review: Extented Polynomial Chaos Expansion

Clearly, the numerical value of $X_{\boldsymbol{\alpha}}$ depends both on the mapping from $\boldsymbol{K}$ to X, and the mapping from $\boldsymbol{\xi}$ to $\boldsymbol{K}$. The former mapping encapsulates physics models and governing equations while the latter mapping describes the probabilistic model of the physical parameters $\boldsymbol{K}$, in a functional form that explicitly relates them to a set of independent Gaussian random variables $\boldsymbol{\xi}$. Uncertainty in the probabilistic model of $\boldsymbol{K}$ is propagated into uncertainty about X through the composite map from $\boldsymbol{K}$ to $\boldsymbol{\xi}$ and $\boldsymbol{\xi}$ to X.

We introduce the m-dimensional vector $\boldsymbol{P} = \{P_1, \cdots, P_m\}$ representing all the statistical parameters of the input random variables $\boldsymbol{K}$. These parameters are typically estimated based on a finite sample. Different estimation methods yield different probabilistic models for $\boldsymbol{P}$ with the Maximum Likelihood estimates (MLE) generally yielding an asymptotically (for large sample size) Gaussian distribution with variance that is inversely proportional to sample size. We represent the random vector $\boldsymbol{P}$ in a polynomial chaos decomposition relative to a new Gaussian germ $\boldsymbol{\rho}$ independent of $\boldsymbol{\xi}$. Motivated by asymptotic results concerning MLE sampling distributions, we limit this PCE to a first order expansion, resulting in a Gaussian

model for $\boldsymbol{P}$. We also assume a one-dimensional PCE representation for $\boldsymbol{P}$, imposing a strict dependence between the different P_i, making them all linear transformations of the same scalar random variable ρ. This statistical dependence between components of $\boldsymbol{P}$ is justified by the observation that experimental evidence that influences our estimate of any one of the P_i's is likely to also affect our estimates of all other components of $\boldsymbol{P}$. We recognize that this dependence assumption can be violated (e.g. the minimum and maximum values of a sample are likely to be independent, as are the sample mean and sample variance). While these violations are the exception, one should be mindful of such occurences. We note that while our proposed formalism can be readily extended to situations where the parameters $\boldsymbol{P}$ are statistically independent by introducing a vector-valued $\boldsymbol{\rho}$ commensurate with $\boldsymbol{P}$, we choose to instead rely on beta random variables in our numerical examples, for which estimators of the shape parameters can be shown to be statistically dependent [37]. We thus introduce ρ as a standard normal random variable independent of $\boldsymbol{\xi} = \{\xi_1, \cdots, \xi_d\}$, and express the parameters of the input PDFs, P_i, in the form,

$$P_i = \mu_{P_i} + \sigma_{P_i}\rho, \;\; i = 1, \cdots, N_P, \tag{6}$$

where μ_{P_i} is the mean of P_i, and σ_{P_i} its standard deviation. Also, N_P denotes the number of parameters from the set $\boldsymbol{P}$ that is presumed to be uncertain.

Thus, X can be represented as a function of a new germ $\boldsymbol{\eta} = \{\xi_1, \cdots, \xi_d, \rho\}$, and is therefore denoted as $X(\boldsymbol{\eta})$. The extended polynomial expansion of X can thus be expressed as,

$$X(\boldsymbol{\eta}) = \sum_{|\boldsymbol{\gamma}| \le p} X_{\boldsymbol{\gamma}} \psi_{\boldsymbol{\gamma}}(\boldsymbol{\eta}) \;, \qquad \boldsymbol{\eta} \in \mathbb{R}^{d+1}, \; \boldsymbol{\gamma} \in \mathbb{N}^{d+1} \tag{7}$$

where $\{X_{\boldsymbol{\gamma}}\}$ denote the PCE coefficients. It is consistent with common views [4, 1, 33, 36, 24, 42, 34] to construe dependence on $\boldsymbol{\xi}$ and $\boldsymbol{\rho}$ to represent, respectively, aleatory and epistemic uncertainties. Eq. (7) provides a joint and uniform representation of these two uncertainties in a single representation. It is worth reiterating that the extension of the foregoing to the case where each P_i is decomposed according to its own stochastic dimension ρ_i can be readily accommodated, with some increase in computational cost.

For a given polynomial order p and germ dimension d, the number of terms in an EPCE, denoted by N_{epce}, is equal to,

$$N_{\text{epce}} = \frac{(d+p+1)!}{(d+1)!\; p!}. \tag{8}$$

4. PCE with Random Coefficients via EPCE

We now construct a prior random model for the PCE coefficients which then gets updated to a posterior model via data assimilation. Making use of Eq. (2), we can separate the dependence on $\boldsymbol{\xi}$ from the dependence on ρ in Eq. (7), resulting in the following representation of EPCE,

$$X(\boldsymbol{\eta}) = X(\boldsymbol{\xi}, \rho) = \sum_{|\boldsymbol{\alpha}| + \beta \le p} X_{\boldsymbol{\alpha}\beta} \psi_{\boldsymbol{\alpha}}(\boldsymbol{\xi}) \psi_{\beta}(\rho), \quad \boldsymbol{\xi} \in \mathbb{R}^d, \; \rho \in \mathbb{R}, \; \boldsymbol{\alpha} \in \mathbb{R}^d, \; \boldsymbol{\beta} \in \mathbb{R}, \tag{9}$$

with the subscript $\boldsymbol{\alpha}\beta$ being a $(d+1)$ multi-index formed as the concatenation of $\boldsymbol{\alpha}$ and β. The result is a PCE whose coefficients are function of ρ, and which can be expressed as,

$$X(\boldsymbol{\xi}; \rho) = \sum_{|\boldsymbol{\alpha}| \le p} X_{\boldsymbol{\alpha}}(\rho) \psi_{\boldsymbol{\alpha}}(\boldsymbol{\xi}) \;, \tag{10}$$

where the PCE coefficients $X_{\boldsymbol{\alpha}}(\rho)$ are now random variables depending on ρ. Noting that not all coefficients $X_{\boldsymbol{\alpha}}$ exhibit dependence on ρ, the PCE in Eq. (10) can be separated into the ρ-dependent and ρ-independent parts resulting in,

$$X(\boldsymbol{\xi}; \rho) = \underbrace{\sum_{|\boldsymbol{\alpha}| < p} X_{\boldsymbol{\alpha}}(\rho) \psi_{\boldsymbol{\alpha}}(\boldsymbol{\xi})}_{\rho\text{-dependent PCE terms}} + \underbrace{\sum_{|\boldsymbol{\alpha}| = p} X_{\boldsymbol{\alpha}} \psi_{\boldsymbol{\alpha}}(\boldsymbol{\xi})}_{\rho\text{-independent PCE terms}} \quad , \quad \boldsymbol{\xi} \in \mathbb{R}^d, \; \rho \in \mathbb{R} \;, \boldsymbol{\alpha} \in \mathbb{N}^d \tag{11}$$

It can be seen that only the highest order PCE coefficients are independent of ρ. Thus, denoting the number of elements in the first and second summations in Eq. (11) by N_{dep} and N_{ind}, respectively, we have

$$\begin{aligned} N_{\text{dep}} &= \frac{(d+p-1)!}{d!\,(p-1)!}\ , \\ N_{\text{ind}} &= \frac{(d+p-1)!}{(d-1)!\,p!}\ . \end{aligned} \tag{12}$$

Clearly, $N_{\text{dep}} + N_{\text{ind}} = N_{\text{pce}}$.

4.1. Representation of Error in EPCE

Sources of uncertainty in the constructed EPCE could be not only due to the probabilistic models of $\boldsymbol{P}$ and $\boldsymbol{K}$, but also to a finite order truncation of the polynomial expansion and finite quadrature levels (or, more generally, limited accuracy in evaluating the coefficients). We denote the true EPCE of QoI as $\tilde{X}(\boldsymbol{\xi};\rho)$ and the error from the constructed EPCE as $\varepsilon_{\text{epce}}$. We then have,

$$\tilde{X}(\boldsymbol{\xi};\rho) = X(\boldsymbol{\xi};\rho) + \varepsilon_{\text{epce}}\ . \tag{13}$$

The numerical error $\varepsilon_{\text{epce}}$ is represented in a PCE analogous to the first summation in Eq.(11). Thus, an error term $\varepsilon_{\boldsymbol{\alpha}}(\rho)$ is added to each PCE coefficient in $X_{\boldsymbol{\alpha}}(\rho)$, where the multi-index $\boldsymbol{\alpha} \in \mathbb{R}^d$ and $0 < |\boldsymbol{\alpha}| < p$. In this fashion, the random PCE coefficients with EPCE error, denoted by $\tilde{Z}_{\boldsymbol{\alpha}}(\rho,\rho_\epsilon)$, are expressed as,

$$\tilde{Z}_{\boldsymbol{\alpha}}(\rho,\rho_\epsilon) = X_{\boldsymbol{\alpha}}(\rho) + \sigma^2_{\boldsymbol{\alpha}}(\rho)\rho_\epsilon, \quad \boldsymbol{\alpha} \in \mathbb{N}^d,\ 0 < |\boldsymbol{\alpha}| < p\ , \tag{14}$$

where the standard deviation $\sigma_{\boldsymbol{\alpha}}(\rho) = 1\% X_{\boldsymbol{\alpha}}(\rho)$ and ρ_ϵ is a standard Gaussian variable (a new stochastic degree of freedom, or germ) which encodes the numerical errors. From the physical perspective, $\tilde{\boldsymbol{Z}}(\rho,\rho_\epsilon) = \left\{\tilde{Z}_{\boldsymbol{\alpha}}(\rho,\rho_\epsilon), 0 < |\boldsymbol{\alpha}| < p\right\}$ accounts for the errors from the probabilistic model of $\boldsymbol{K}$ and the probabilistic model of $\boldsymbol{P}$, as well as errors in the numerical approximation of the PCE coefficients (quadrature and truncation errors).

Substituting Eq. (14) into Eq. (11) to represent Eq. (13) results in,

$$\tilde{X}(\boldsymbol{\xi};\rho) = X_0(\rho) + \sum_{0<|\boldsymbol{\alpha}|<p} \tilde{Z}_{\boldsymbol{\alpha}}(\rho,\rho_\epsilon)\psi_{\boldsymbol{\alpha}}(\boldsymbol{\xi}) + \sum_{|\boldsymbol{\alpha}|=p} X_{\boldsymbol{\alpha}}\psi_{\boldsymbol{\alpha}}(\boldsymbol{\xi})\ , \tag{15}$$

In our construction, the numerical errors considered (quadrature and truncation errors) in EPCE do not affect the mean of QoI but only the higher-order statistics. The error terms generate scatter around the "mode" which is the relationship obtained by EPCE. In other words, the mode of the prior is constructed from EPCE and we add an additive Gaussian error which induces a small statistical perturbation around this mode. In this manner, the prior constructed is physcially informative. When observations are acquired, Eq. (15) is the model that we aim to update in which $\tilde{\boldsymbol{Z}}(\rho,\rho_\epsilon) = \left\{\tilde{Z}_{\boldsymbol{\alpha}}(\rho,\rho_\epsilon), \boldsymbol{\alpha} \in \mathbb{N}^d, 0 < |\boldsymbol{\alpha}| < p\right\}$ are the parameters to infer. The ρ-independent part participates in the inverse analysis while $\{X_{\boldsymbol{\alpha}}, |\boldsymbol{\alpha}| = p\}$ remain deterministic during the analysis.

To explicitly represent the error term, Eq. (15) can be equivalently written as,

$$\tilde{X}(\boldsymbol{\xi};\rho) = X_0(\rho) + \sum_{0<|\boldsymbol{\alpha}|<p} X_{\boldsymbol{\alpha}}(\rho)\psi_{\boldsymbol{\alpha}}(\boldsymbol{\xi}) + \underbrace{\sum_{0<|\boldsymbol{\alpha}|<p} \sigma^2_{\boldsymbol{\alpha}}(\rho)\rho_\epsilon\psi_{\boldsymbol{\alpha}}(\boldsymbol{\xi})}_{\text{error term}} + \sum_{|\boldsymbol{\alpha}|=p} X_{\boldsymbol{\alpha}}\psi_{\boldsymbol{\alpha}}(\boldsymbol{\xi})\ . \tag{16}$$

In Eqs. (15) or (16), sensitivities with respect to model parameters can be readily evaluated by differentiation. Sensitivity with respect to other parameters (either input, or latent, or output quantities) can be approximated by considering directional derivatives in the direction of the dominant germs for these quantities. This aspect of the analysis is not in the scope of the present paper.

5. Bayesian Inference

Let us assume N_D number of observations $\boldsymbol{D} = (D^{(1)}, D^{(2)}, \cdots, D^{(N_D)})$ are acquired. The task is to calibrate the prediction model to make more accurate predictions. The "model" can be either the physical model (e.g., a finite element code) or the surrogate model (e.g., a PCE). In this section, we perform Bayesian model updating for both cases.

5.1. Standard Bayesian Inference

The standard Bayesian inference is to update the physical parameters $\boldsymbol{K}$ in the physics model. In this case, the Bayes's theorem is written as,

$$f_{\boldsymbol{K}|\boldsymbol{D}}(\boldsymbol{k}, \boldsymbol{\mathcal{D}}) = C_s L_s(\boldsymbol{k}, \boldsymbol{\mathcal{D}}) f_{\boldsymbol{K}}(\boldsymbol{k}) \ , \tag{17}$$

where, $f_K(\boldsymbol{k})$ is the prior distribution of $\boldsymbol{K}$; $f_{\boldsymbol{K}|\boldsymbol{D}}(\boldsymbol{k}, \boldsymbol{\mathcal{D}})$ represents the posterior distribution of $\boldsymbol{K}$; $L_s(\boldsymbol{k}, \boldsymbol{\mathcal{D}})$ is the likelihood function given observations $\boldsymbol{\mathcal{D}}$; and C_s is a normalizing constant.

To account for the physical model error, an additive Gaussian representation is typically used which is expressed as,

$$\tilde{X}(\boldsymbol{K}) = X(\boldsymbol{K}) + \mathcal{N}(0, \sigma_M^2) \ , \tag{18}$$

where $\tilde{X}(\boldsymbol{K})$ and $X(\boldsymbol{K})$ denote the values of QoI evaluated at $\boldsymbol{K}$ by the true physics and the physics model, respectively. The discrepancy between $\tilde{X}(\boldsymbol{K})$ and $X(\boldsymbol{K})$ characterizes the model error which is represented by a Gaussian distribution with zero mean and standard deviation of σ_M . Thus, the likelihhod function can be represented by,

$$L_s(\boldsymbol{k}, \boldsymbol{\mathcal{D}}) = \prod_{m=1}^{N_D} \frac{1}{\sigma_M \sqrt{2\pi}} \exp\left(-\frac{1}{2} \left(\frac{\mathcal{D}^{(m)} - X(\boldsymbol{k})}{\sigma_M} \right)^2 \right) \ . \tag{19}$$

5.2. Bayesian Inference for Random PCE coefficients

The Bayesian inference can be also applied to calibrate the PCE surrogate model in Eq. (15). In this case, the parameters to infer are the random PCE coefficients. Sampling ρ and ρ_ϵ gives realizations of the prior random coefficients $\tilde{\boldsymbol{Z}}(\rho, \rho_\epsilon) = \left\{ \tilde{Z}_{\boldsymbol{\alpha}}(\rho, \rho_\epsilon), \boldsymbol{\alpha} \in \mathbb{N}^d, 0 < |\boldsymbol{\alpha}| < p \right\}$ as constructed in Section (4.1). Once the prior is built, we do not consider ρ or ρ_ϵ any more. Thus, the posterior of these random PCE coefficients denoted by $\tilde{\boldsymbol{Z}}|\boldsymbol{D} = \left\{ \tilde{Z}_{\boldsymbol{\alpha}}|\boldsymbol{D}, \boldsymbol{\alpha} \in \mathbb{N}^d, 0 < |\boldsymbol{\alpha}| < p \right\}$ does not depend on ρ or ρ_ϵ. The Bayes's theorem applied on $\tilde{\boldsymbol{Z}}$ is thus represented by,

$$f_{\tilde{\boldsymbol{Z}}|\boldsymbol{D}}(\tilde{\boldsymbol{z}}, \boldsymbol{\mathcal{D}}) = C L(\tilde{\boldsymbol{z}}, \boldsymbol{\mathcal{D}}) f_{\tilde{\boldsymbol{Z}}}(\tilde{\boldsymbol{z}}) \ , \tag{20}$$

where, $f_{\tilde{\boldsymbol{Z}}}(\tilde{\boldsymbol{z}})$ is the prior distribution which is a joint distribution of $\tilde{\boldsymbol{Z}}(\rho, \rho_\epsilon)$; $f_{\tilde{\boldsymbol{Z}}|\boldsymbol{D}}(\tilde{\boldsymbol{z}}, \boldsymbol{\mathcal{D}})$ represents the posterior distribution which is a joint distribution of the PCE coefficients after calibration based on $\boldsymbol{\mathcal{D}}$; $L(\tilde{\boldsymbol{z}}, \boldsymbol{\mathcal{D}})$ is the likelihood function given observations $\boldsymbol{\mathcal{D}}$; and C is a normalizing constant.

5.2.1. Prior

The samples of prior can be directly obtained by sampling ρ and ρ_ϵ and mapping them into samples of $\tilde{\boldsymbol{Z}}(\rho, \rho_\epsilon)$. Then the joint prior distribution $f_{\tilde{\boldsymbol{Z}}}(\tilde{\boldsymbol{z}})$ can be estimated by the multivariate kernel density estimation (KDE) using these prior samples, which can be expressed as,

$$f_{\tilde{\boldsymbol{Z}}}(\tilde{\boldsymbol{z}}) = \frac{1}{N_\rho |\boldsymbol{H}_1|^{1/2}} \sum_{j=1}^{N_\rho} K_H \left(\boldsymbol{H}_1^{-1/2} \left(\tilde{\boldsymbol{z}} - \tilde{\boldsymbol{Z}}(\rho^{(j)}, \rho_\epsilon^{(j)}) \right) \right) \ , \tag{21}$$

where K_H is the kernel function which is a symmetric multivariate density; $\boldsymbol{H}_1 \in \mathbb{R}^{N_{\text{dep}}} \times \mathbb{R}^{N_{\text{dep}}}$ is the bandwidth matrix which is symmetrix and positive definite; $\tilde{\boldsymbol{Z}}(\rho^{(j)}, \rho_\epsilon^{(j)})$ is the j-th sample of $\tilde{\boldsymbol{Z}}(\rho, \rho_\epsilon)$; and N_ρ is the number of PCE samples used to estimate the multivariate KDE.

5.2.2. Likelihood

The likelihood function is given by,

$$L(\tilde{\boldsymbol{z}}, \boldsymbol{\mathcal{D}}) = \prod_{m=1}^{N_D} f_X\left(\mathcal{D}^{(m)}|X(\tilde{\boldsymbol{z}})\right) , \tag{22}$$

where $f_X\left(\cdot|X(\tilde{\boldsymbol{z}})\right)$ denotes the response PDF estimated by PCE as a function of $\tilde{\boldsymbol{Z}}(\rho, \rho_\epsilon)$. Then, $f_X\left(\mathcal{D}^{(m)}|X(\tilde{\boldsymbol{z}})\right)$ is the value of the response PDF evaluated at an observation $\mathcal{D}^{(m)}$. In other words, the likelihood function and response PDF are both stochastic models depending on ρ and ρ_ϵ.

5.2.3. Posterior

According to Bayes' theorem as expressed in Eq. (20), combined with Eqs. (21) and (22), the posterior is expressed as,

$$f_{\tilde{\boldsymbol{Z}}|\boldsymbol{D}}(\tilde{\boldsymbol{z}}, \boldsymbol{\mathcal{D}}) = \frac{C}{N_\rho |\boldsymbol{H}_1|^{1/2}} \prod_{m=1}^{N_D} f_X\left(\mathcal{D}^{(m)}|X(\tilde{\boldsymbol{z}})\right) \sum_{j=1}^{N_\rho} K_H\left(\boldsymbol{H}_1^{-1/2}\left(\tilde{\boldsymbol{z}} - \tilde{\boldsymbol{Z}}(\rho^{(j)}, \rho_\epsilon^{(j)})\right)\right) , \tag{23}$$

5.2.4. Metropolis-Hastings Algorithm

We use the Metropolis-Hastings algorithm to sample from the posterior. The pseudocode is shown in Algorithm 1. It is worth mentioning that the model evaluations in associated Markov chains are performed by the PCE surrogate model that has been built in Section 4, and the Bayesian procedure thus has little numerical efforts.

After posterior samples are collected, the multivariate KDE is used to estimate the joint posterior PDF of PCE coefficients, which results in,

$$f_{\tilde{\boldsymbol{Z}}|\boldsymbol{D}}(\tilde{\boldsymbol{z}}, \boldsymbol{\mathcal{D}}) = \frac{1}{N_a |\boldsymbol{H}_2|^{1/2}} \sum_{j'=1}^{N_a} K_H\left(\boldsymbol{H}_2^{-1/2}\left(\tilde{\boldsymbol{z}}|\boldsymbol{\mathcal{D}} - \tilde{\boldsymbol{Z}}^{(j')}|\boldsymbol{D}\right)\right) , \tag{24}$$

where $\tilde{\boldsymbol{Z}}^{(j')}|\boldsymbol{D}$ is the j'-th posterior sample; K_H is the kernel function which is a symmetric multivariate density; $\boldsymbol{H}_2 \in \mathbb{R}^{N\text{dep}} \times \mathbb{R}^{N\text{dep}}$ is the bandwidth matrix which is symmetric and positive definite; N_a is the number of accepted samples of the posterior used in multivariate KDE.

6. Stochastic Models for PDFs

When we use the posterior random PCE coefficients $\tilde{\boldsymbol{Z}}|\boldsymbol{D}$ to build the PCE, the updated PCE representation of QoI denoted by $\tilde{X}|\boldsymbol{D}$ is a function of the random vector $\tilde{\boldsymbol{Z}}|\boldsymbol{D} = \left\{\tilde{Z}_{\boldsymbol{\alpha}}|\boldsymbol{D}, \boldsymbol{\alpha} \in \mathbb{N}^d, 0 < |\boldsymbol{\alpha}| < p\right\}$ with only the mean dependent on ρ, expressed as,

$$\tilde{X}|\boldsymbol{D}(\boldsymbol{\xi}, \tilde{\boldsymbol{Z}}|\boldsymbol{D}, \rho) = X_0(\rho) + \sum_{0<|\boldsymbol{\alpha}|<p} \tilde{Z}_{\boldsymbol{\alpha}}|\boldsymbol{D}\ \psi_{\boldsymbol{\alpha}}(\boldsymbol{\xi}) + \sum_{|\boldsymbol{\alpha}|=p} X_{\boldsymbol{\alpha}} \psi_{\boldsymbol{\alpha}}(\boldsymbol{\xi}) , \tag{25}$$

A stochastic model for the PDF of X is used to characterize confidence in estimates of failure probability. The PDF of QoI computed by PCEs with prior and posterior random PCE coefficients $\tilde{\boldsymbol{Z}}(\rho, \rho_\epsilon)$ and $\tilde{\boldsymbol{Z}}|\boldsymbol{D}$ are random variables and can be expressed as,

$$\begin{aligned} f_X\left(x, \tilde{\boldsymbol{Z}}(\rho, \rho_\epsilon)\right) &= \frac{1}{N_\rho h_1} \sum_{j=1}^{N_\rho} K_h\left(\frac{x - \tilde{X}\left(\boldsymbol{\xi}^{(j)}, \tilde{\boldsymbol{Z}}(\rho, \rho_\epsilon)\right)}{h_1}\right) ; \\ f_X(x, \tilde{\boldsymbol{Z}}|\boldsymbol{D}, \rho) &= \frac{1}{N_a h_2} \sum_{j'=1}^{N_a} K_h\left(\frac{x - \tilde{X}|\boldsymbol{D}(\boldsymbol{\xi}^{(j')}, \tilde{\boldsymbol{Z}}|\boldsymbol{D}, \rho)}{h_2}\right) , \end{aligned} \tag{26}$$

Algorithm 1 Metropolis-Hastings posterior sampler for PCE coefficients

function TARGET($\tilde{\boldsymbol{z}}^{(s)}$) ▷ Input is a sample of prior random PCE coefficients
  $L(\tilde{\boldsymbol{z}}^{(s)}, \boldsymbol{\mathcal{D}}) \leftarrow \prod_{m=1}^{N_D} f_X\big(\mathcal{D}^{(m)} | X(\tilde{\boldsymbol{z}}^{(s)})\big)$
  $\pi(\tilde{\boldsymbol{z}}^{(s)}) \leftarrow L(\tilde{\boldsymbol{z}}^{(s)}, \boldsymbol{\mathcal{D}}) f_{\tilde{\boldsymbol{Z}}}(\tilde{\boldsymbol{z}}^{(s)})$
  return $\pi(\tilde{\boldsymbol{z}}^{(s)})$ ▷ Output is a scalar
end function

function PROPOSAL($\tilde{\boldsymbol{z}}^{(s)}$) ▷ Define proposal distribution
  $\tilde{\boldsymbol{z}}^{(s)} \sim$ Multivariate normal$(\tilde{\boldsymbol{z}}^{(s)}, \boldsymbol{\Sigma})$ ▷ $\boldsymbol{\Sigma}$ is covariance matrix
  return $\tilde{\boldsymbol{z}}^{(s+1)}$
end function

Initialization: Choose any sample of $\tilde{\boldsymbol{z}}^{(0)}$ from prior;
for $s \leftarrow 1$ to N_s **do** ▷ N_s is the number of MCMC steps
  $\tilde{\boldsymbol{z}}^{(s+1)} \sim$ PROPOSAL$(\tilde{\boldsymbol{z}}^{(s)})$
  $\pi(\tilde{\boldsymbol{z}}^{(s)}) \leftarrow$ TARGET$(\tilde{\boldsymbol{z}}^{(s)})$
  $\pi(\tilde{\boldsymbol{z}}^{(s+1)}) \leftarrow$ TARGET$(\tilde{\boldsymbol{z}}^{(s+1)})$
  $R^{(s)} \leftarrow \min\big\{\frac{\pi(\tilde{\boldsymbol{z}}^{(s+1)})}{\pi(\tilde{\boldsymbol{z}}^{(s)})}, 1\big\}$
  $u^{(s)} \sim$ Uniform(0, 1)
  if $R^{(s)} \geq u^{(s)}$ **then**
    accept $\tilde{\boldsymbol{z}}^{(s+1)}$
    $\tilde{\boldsymbol{z}}^{(s+1)} \leftarrow \tilde{\boldsymbol{z}}^{(s+1)}$
  else
    reject $\tilde{\boldsymbol{z}}^{(s+1)}$
    $\tilde{\boldsymbol{z}}^{(s+1)} \leftarrow \tilde{\boldsymbol{z}}^{(s)}$
  end if
end for
return accepted samples ▷ Collect posterior samples

where Gaussian kernel is used for K_h with the bandwidth h_1 and h_2 determined following Silverman's rule [43] as $h_1 = (4\sigma_1^5/3N_\rho)^{1/5}$ and $h_2 = (4\sigma_2^5/3N_a)^{1/5}$, where σ_1 and σ_2 are the standard deviations estimated from the N_ρ and N_a samples of QoI, respectively. Again, the samples used in Eq. (26) are evaluated by the PCE surrogate model before and after update, respectively, given by,

$$\begin{aligned} \tilde{X}(\boldsymbol{\xi};\rho) &= X_0(\rho) + \sum_{0<|\boldsymbol{\alpha}|<p} \tilde{Z}_{\boldsymbol{\alpha}}(\rho,\rho_\epsilon)\psi_{\boldsymbol{\alpha}}(\boldsymbol{\xi}) + \sum_{|\boldsymbol{\alpha}|=p} X_{\boldsymbol{\alpha}}\psi_{\boldsymbol{\alpha}}(\boldsymbol{\xi}) \ ; \\ \tilde{X}|\boldsymbol{D}(\boldsymbol{\xi},\tilde{\boldsymbol{Z}}|\boldsymbol{D},\rho) &= X_0(\rho) + \sum_{0<|\boldsymbol{\alpha}|<p} \tilde{Z}_{\boldsymbol{\alpha}}|\boldsymbol{D}\ \psi_{\boldsymbol{\alpha}}(\boldsymbol{\xi}) + \sum_{|\boldsymbol{\alpha}|=p} X_{\boldsymbol{\alpha}}\psi_{\boldsymbol{\alpha}}(\boldsymbol{\xi}) \ . \end{aligned} \tag{27}$$

One important application of the aforementioned ideas is to the characterization of failure probabilities, themselves, as random variables. In many applications, the failure probability P_f is defined as the probability of reaching or exceeding a critical threshold and is of great significance. This distribution is typically predicated on pre-specified probabilistic models for input parameters, and thus lends itself to the present analysis. To simplify the presentation, and without loss of generality, we assume a scalar description of the limit state in terms of a critical threshold for the QoI, denoted by X_c. The prior and posterior failure probabilities denoted by P_{f1} and P_{f2}, respectively, are then given by the following integral,

$$\begin{aligned} P_{f1}\big(\tilde{\boldsymbol{Z}}(\rho,\rho_\epsilon)\big) &= \int_{x\geq X_c} f_X\big(x,\tilde{\boldsymbol{Z}}(\rho,\rho_\epsilon)\big)\,dx \ ; \\ P_{f2}(\tilde{\boldsymbol{Z}}|\boldsymbol{D},\rho) &= \int_{x\geq X_c} f_X(x,\tilde{\boldsymbol{Z}}|\boldsymbol{D},\rho)\,dx \ , \end{aligned} \tag{28}$$

where we have explicitly expressed the dependence of P_{f1} and P_{f2} on the prior and posterior random PCE coefficients $\tilde{\boldsymbol{Z}}(\rho,\rho_\epsilon)$ and $\tilde{\boldsymbol{Z}}|\boldsymbol{D}$, respectively. Then, the PDF of P_{f1} and P_{f2} computed by KDE is expressed as,

$$\begin{aligned} f_{P_{f1}}(x) &= \frac{1}{N_\rho h_{f1}} \sum_{j=1}^{N_\rho} K_h\left(\frac{x - P_{f1}\big(\tilde{\boldsymbol{Z}}(\rho^{(j)},\rho_\epsilon^{(j)})\big)}{h_{f1}}\right) \ ; \\ f_{P_{f2}}(x) &= \frac{1}{N_a h_{f2}} \sum_{j'=1}^{N_a} K_h\left(\frac{x - P_{f2}(\tilde{\boldsymbol{Z}}^{(j')}|\boldsymbol{D},\rho^{(j')})}{h_{f2}}\right) \ , \end{aligned} \tag{29}$$

where $f_{P_{f1}}(x)$ and $f_{P_{f2}}(x)$ are the prior and posterior PDFs of failure probabilities P_{f1} and P_{f2}. The Gaussian kernel is used for K_h with the bandwidth h_{f1} and h_{f2} determined following Silverman's rule as $h_{f1} = (4\sigma_{f1}^5/3N_\rho)^{1/5}$ and $h_{f2} = (4\sigma_{f2}^5/3N_a)^{1/5}$, where σ_{f1} and σ_{f2} are the standard deviations estimated from the N_ρ and N_a samples of failure probability, respectively.

7. Case studies

In this section, two examples are investigated to demonstrate the proposed approach. Example I is a beam structure of which a closed-form expression for the QoI is known. Example II is a reinforced concrete wall on which the hysteresis analysis is performed using finite elements.

7.1. Example I: Beam structure

The beam structure is shown in Fig. 1. The model characterizes the mid-span displacement X_{mid} of the beam fixed by a linear spring and a rotational spring at each end, with concentrated load F acting in the middle of the beam. The random inputs include the linear spring, rotational spring, flexural stiffness and beam span, which are denoted as k_1, k_2, EI and L, respectively. It can be shown from elementary mechanics of materials that mid-span displacement X_{mid} for this beam is given by,

$$X_{\text{mid}} = \frac{F}{16EI}\left[\frac{L^3}{3} - \frac{8EIk_2L^3 + k_1k_2L^6}{16EI(k_2+k_1L^2)} + \frac{8EIk_1L^2 - k_1k_2L^3}{2k_1k_2 + 2k_1^2L^2}\right]. \tag{30}$$

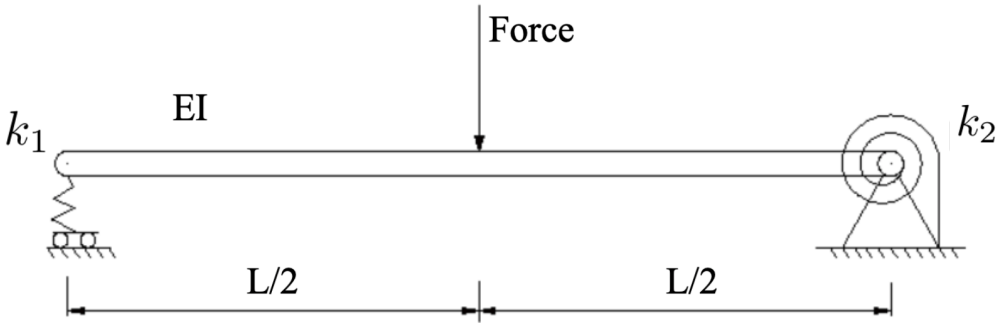

Figure 1: Schematic of the physical setup for Example I: Random beam on random supports.

Table 1: Statistical parameters of random inputs for Example I: beam structure

Input variables	Distribution	$\boldsymbol{a}$	$\boldsymbol{b}$	$\boldsymbol{q}$(fixed)	$\boldsymbol{r}$ (fixed)
Linear spring k_1 (N*m)	Beta	4	5	350	650
Rotational spring k_2 (N*m/rad)	Beta	4	5	400	600
Flexural stiffness EI (N/m*m)	Beta	4	5	80	186.67
Beam span L (m)	Beta	4	5	0.216	0.264

The four input variables, k_1, k_2, EI and L, are mutually independent and follow the Beta distributions. The vector of random statistical parameters $\boldsymbol{P}$ consists of the eight random variables $\boldsymbol{a}$ and $\boldsymbol{b}$ which are the vectors of two shape parameters of the Beta distribution while the lower and upper bounds are fixed. The statistical parameters are listed in Tab. 1. The mean value of $\boldsymbol{P}$ is taken equal to the nominal values, and the coefficient of variation of each entry in $\boldsymbol{P}$ is assumed to 5%.

From the EPCE, the mean of predicted response PDF is 2.09 cm. We assume 10 artificial observations generated from a uniform distribution with bounds of (2.4, 2.6), which gives
$\boldsymbol{\mathcal{D}} = \{2.42, 2.43, 2.58, 2.55, 2.41, 2.51, 2.54, 2.50, 2.54, 2.43\}$ cm.

A second order EPCE was found to be sufficiently converged in the response PDF to carry out the foregoing studies. Thus, in the stochastic PCE constructed in Section 4, only the 0th-order and 1st-order PCE coefficients are random ($N_r = 5$).

The results of Bayesian inference on the coefficients of the PCE surrogate model are plotted. Fig. 2 shows the statistics of the random PCE coefficients directly build by EPCE according to Eq. (10), and the statistics of the joint prior of the random PCE coefficients that includes the error terms according to Eq. (21). It indicates that the terms representing the error in EPCE generate scatter around the "mode" which is a deterministic relationship obtained by EPCE. Fig. 3 depicts the statistics of the joint posterior of the random PCE coefficients including the samples (lower left), marginal PDFs (diagonal) and joint PDFs (upper right), according to Eq. (24). The posterior samples have larger scatter compared to the prior. Fig. 4 exhibits the family of predicted PDF of QoI using prior and posterior PCE models in Eq. (26). It is found that the posterior PDF family is thinner than the prior family, which indicates that the posterior predictions have smaller scatter than the prior predictions. Assuming failure is associated with $X_{\text{mid}} > 2.45$cm, the distribution of the probability of failure P_f is obtained by evaluating P_f for each sample in Fig. 4, and plotting the PDF of the resulting values, according to Eq. (29). The resulting PDFs from prior and posterior are shown in Fig. 5. The posterior distribution of failure probability is sharper than the prior prediction and shifts to the right, which indicates that the observations improve the credibility of the prediction and an increase in overall failure probability is forecasted.

Standard Bayesian inference is also conducted on the physical parameters $\boldsymbol{K}$ in the physics model of the beam in Eq. (30). Fig. 6 shows the prior and posterior distributions of $\boldsymbol{K}$ when the Gaussian noise in the likelihood $\sigma_M = 30\%$. The prior of $\boldsymbol{K}$ corresponds to $\rho = 0$ in EPCE and the posterior of $\boldsymbol{K}$ provides the best $\boldsymbol{P}$ in consistence of the observations.

For a clear comparison of the two Bayesian approaches, the prior and posterior predictions of QoI by updating $\boldsymbol{K}$ and $\tilde{\boldsymbol{Z}}(\rho, \rho_\epsilon)$ are plotted together in Fig. 7. It shows that the update of $\boldsymbol{K}$ induces a shift of the response PDF and a change in shape. For the update of $\tilde{\boldsymbol{Z}}(\rho, \rho_\epsilon)$, shift in the family of response PDFs is not observed while the PDFs ensemble is narrower. Such influence is also reflected in the distribution of failure probability as a shift and change in the shape of its PDF. This is due to the fact that, a sample of PCE coefficients generates a full response PDF by the corresponding PCE surrogate model while a sample of physical parameters composes a physics model which predicts a value of QoI. That is to say, the PCE coefficients contain more information (i.e. probabilistic information) than the physical parameters. The inference of PCE coefficients thus allows a dual-level characterization of the uncertainty in QoI, which is more informative.

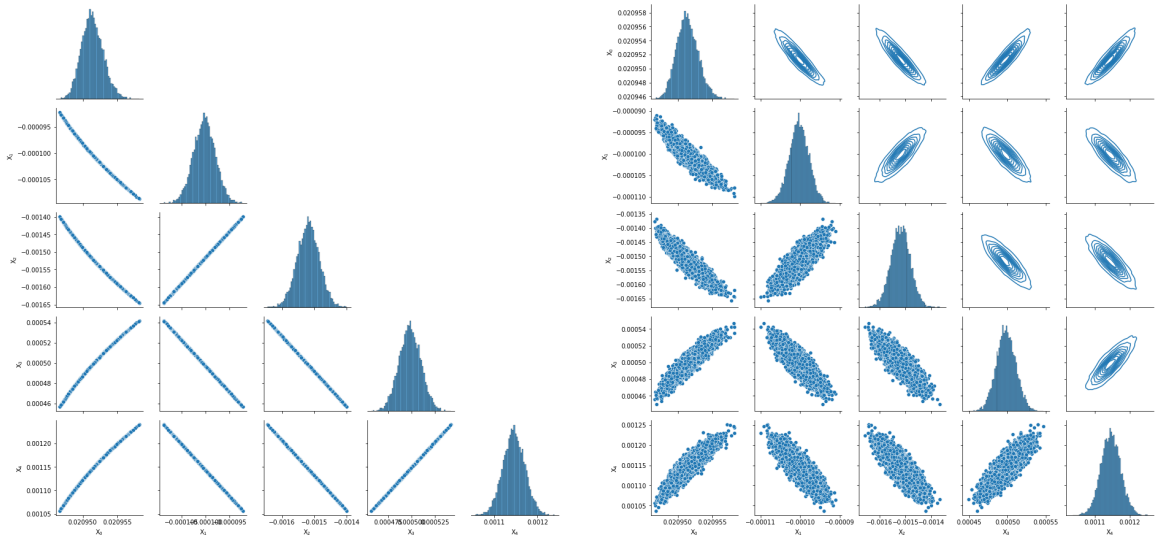

Figure 2: Comparison of statistics of the prior PCE coefficients directly from EPCE (left) and the prior PCE coefficients with error term (right) in Example I.

7.2. Example II: Reinforced concrete shear wall

Many literatures have suggested that epistemic uncertainty is non-ignorable in dynamic analysis of structures [44, 45, 46, 47, 48]. To demonstrate the proposed methodologies in this context, a reinforced concrete shear wall model is investigated in this study. This model comes from an experimental study [49]. Fig. 8 depicts the geometry, dimension and reinforcement of the shear wall.

There are two steps in the loading procedure. First, a constant axial load of 378 kN is applied on the top of the wall, followed by a cyclic lateral load achieved by controlling the displacement. The applied lateral drift consisted of a train of triangular pulses of alternating signs. Additional details of the setup and its loading are described elsewhere [49]. The purpose of the present analysis is to find the influence of the statistical parameters of mechanical properties of concrete and steel on the response PDF of the energy dissipated throughout the structure via hysteresis.

Some of the material properties are considered as random variables, including the concrete elastic modulus E_c, the concrete tensile strength f_r, the concrete compressive strength f_c and the steel yielding strength f_y. For concrete, E_c, f_r and f_c are of course correlated, but for simplicity they were regarded as fully correlated in this paper. According to the code ACI 318-19 [50], the relationships between these parameters are,

$$\begin{aligned} E_c &= 57,000\sqrt{f_c} \quad , \\ f_r &= 7.5\lambda\sqrt{f_c} \quad , \end{aligned} \tag{31}$$

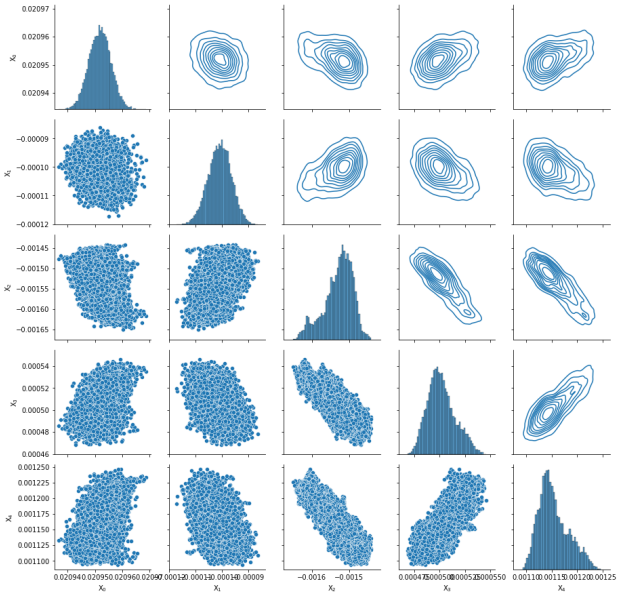

Figure 3: Posterior distribution of PCE coefficients in Example I.

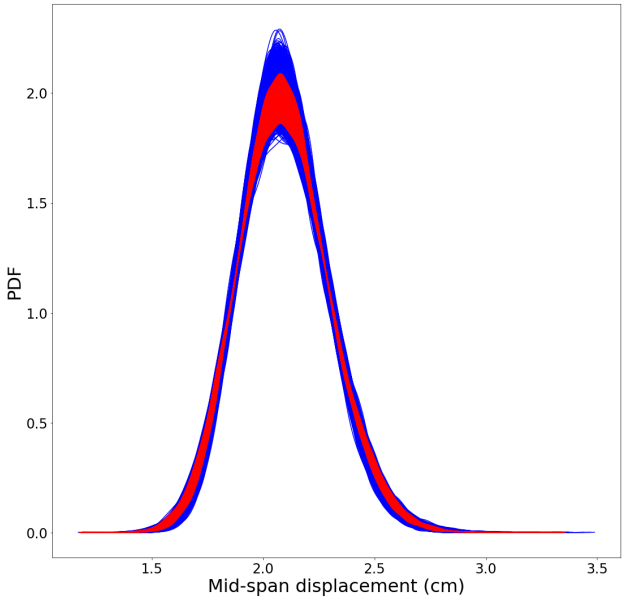

Figure 4: The family of response PDFs computed by posterior PCEs (red) and the family by prior PCEs (blue) in Example I.

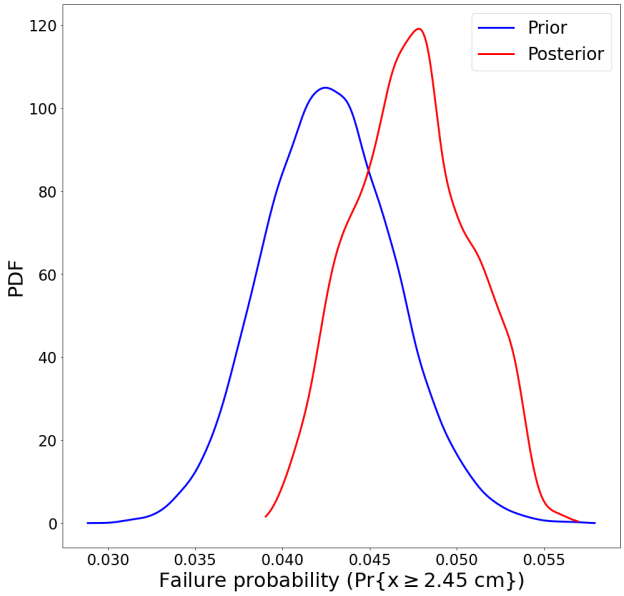

Figure 5: The posterior and prior distributions of the probability of failure in Example I.

Table 2: Statistical parameters of random inputs for Example II: reinforced concrete shear wall

Material	Input variable	Distribution	$\boldsymbol{a}^{SW}$	$\boldsymbol{b}^{SW}$	$\boldsymbol{q}^{SW}$ (fixed)	$\boldsymbol{r}^{SW}$ (fixed)
Concrete	Compressive strength f_c (in Pa)	Beta	2	2	3.91×10^7	5.29×10^7
Steel	Yielding strength f_y (in Pa)	Beta	2	2	3.40×10^8	4.60×10^8

where, the units are in psi. To calculate these concrete parameters, the f_c is sampled from a Beta distribution first and the f_r and E_c are then generated according to Eq. 31. The steel strength is also modeled as a Beta random input. The material properties input to the shear wall structure are listed in Tab. 2. where, in this shear wall hysteresis problem, $\boldsymbol{a}^{SW}$ and $\boldsymbol{b}^{SW}$ are the vectors of two shape parameters of each input from the original dataset; $\boldsymbol{q}^{SW}$ and $\boldsymbol{r}^{SW}$ are the vectors of the lower and upper bounds of each input and assumed to be the same in any dataset. Thus, in this example, the vector $\boldsymbol{P}$ of random parameters has four components consisting of the shape parameters $\boldsymbol{a}^{SW}$ and $\boldsymbol{b}^{SW}$. The mean value of $\boldsymbol{P}$ is taken equal to the values estimated from the original dataset, and the coefficient of variation of each entry in $\boldsymbol{P}$ is assumed to 5%.

We implement in Abaqus [51] a model that follows the theoretical development in Feng et.al [52] which features a multi-dimensional softened plasticity damage model. The steel material follows a Menegotto-Pinto model that includes strain-hardening, Baushinger effects and tension stiffening and a multi-layer shell element is used for the shear wall [52]. Additional material properties include the concrete Poisson's ratio, the steel elastic modulus and the steel hardening ratio which are deterministic inputs.

A second order EPCE was found to be sufficiently converged in the response PDF to carry out the foregoing studies. In such case, the 0th-order and 1st-order PCE coefficients are random in the stochastic PCE constructed in Section 4, and $N_r = 3$.

Since the assessment and comparison of standard Bayesian analysis of physics parameters have been discussed in details using Example I, we focus on applying the proposed approach in this example. The statistics of the random PCE coefficients directly built by EPCE according to Eq. (10), and the joint prior of these coefficients that includes the EPCE error terms according to Eq. (21) are plotted in Fig. 9. Again, EPCE provides the deterministic relationships as the "modes" and the error terms generate scatter around these modes. Using the Bayesian inference, the statistics of the joint posterior of the random PCE

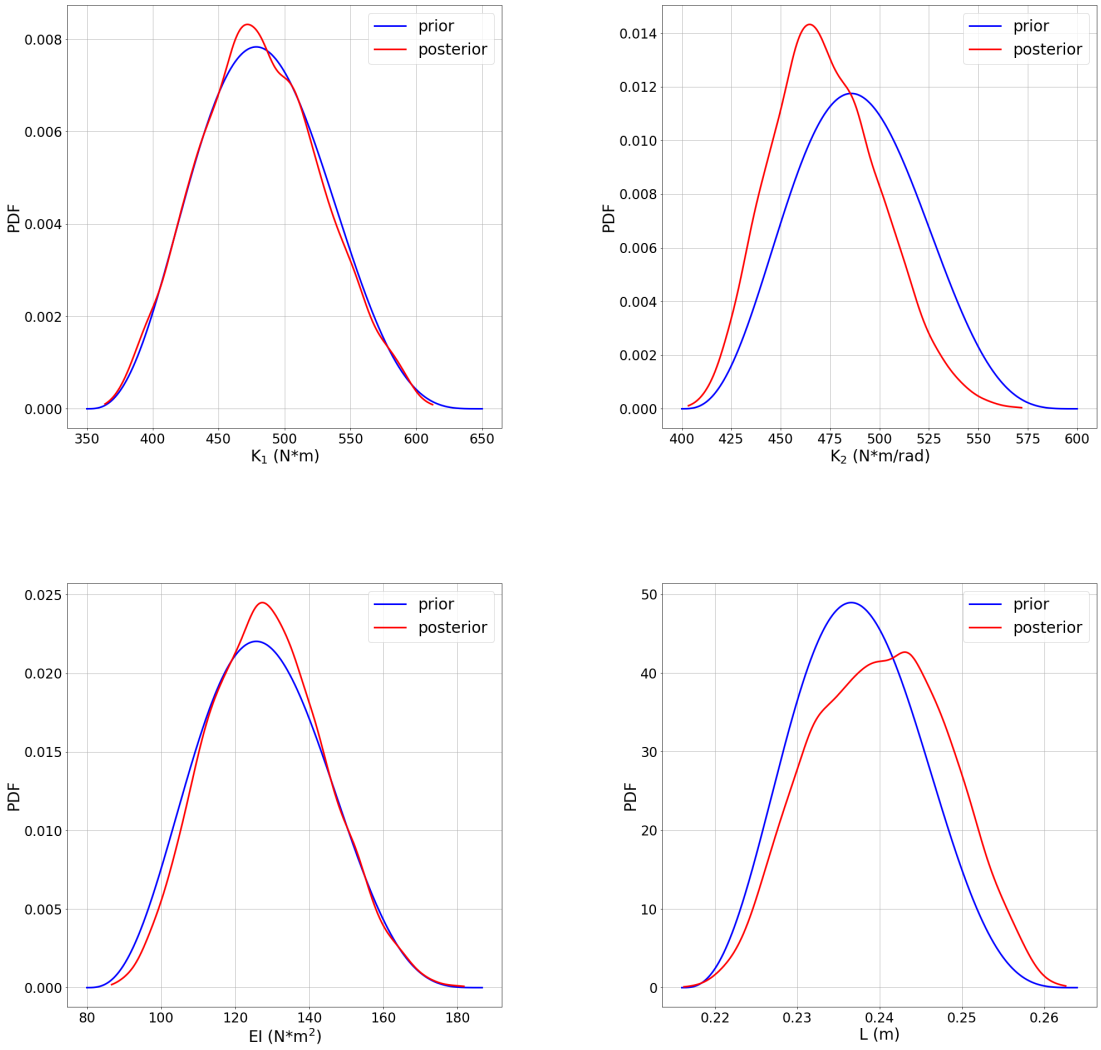

Figure 6: The posterior and prior distributions of $\boldsymbol{K}$ by standard Bayesian inference ($\sigma_M = 30\%$) in Example I.

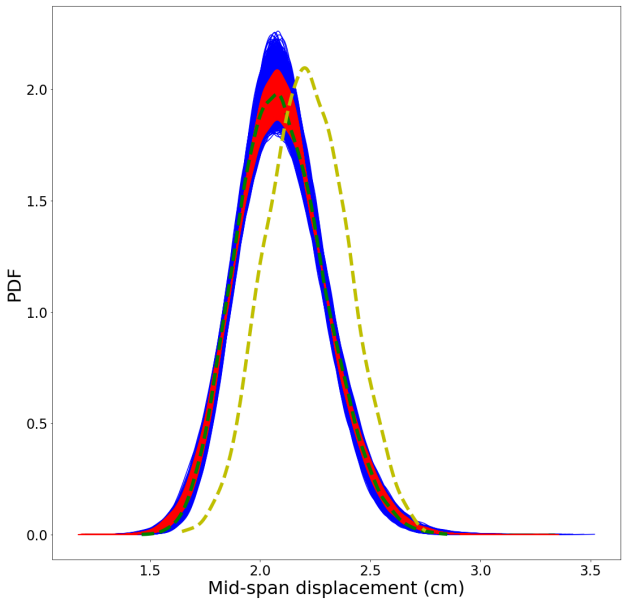

Figure 7: The family of response PDFs computed by posterior PCEs (red); the family by prior PCEs (blue); prior (dashed green) and posterior (dashed yellow) PDFs of QoI by standard Bayesian inference of $\boldsymbol{K}$ ($\sigma_M = 30\%$) in Example I.

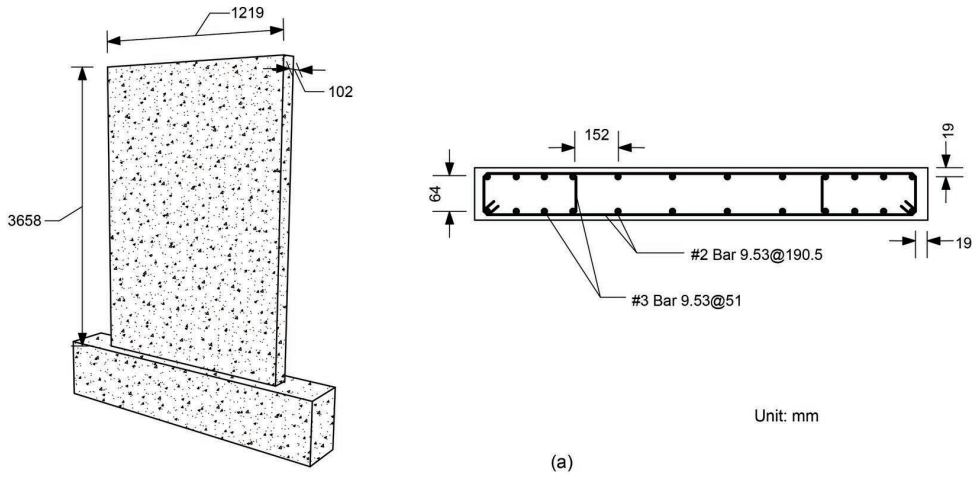

Figure 8: Schematic of the physical setup for Example II: Reinforced concrete shear wall.

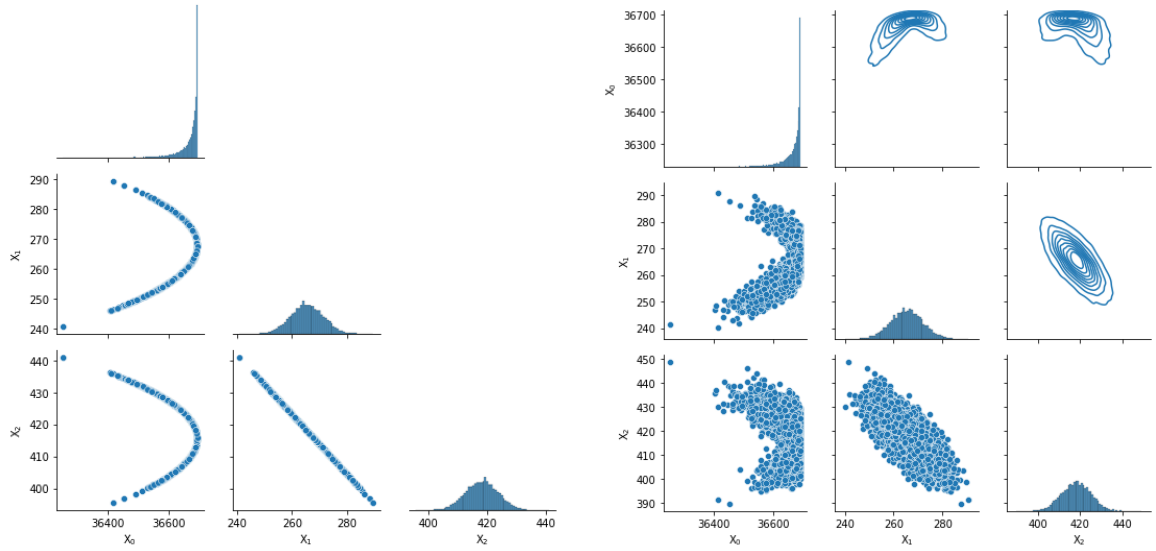

Figure 9: Comparison of statistics of the prior PCE coefficients directly from EPCE (left) and the prior PCE coefficients with error term (right) in Example II.

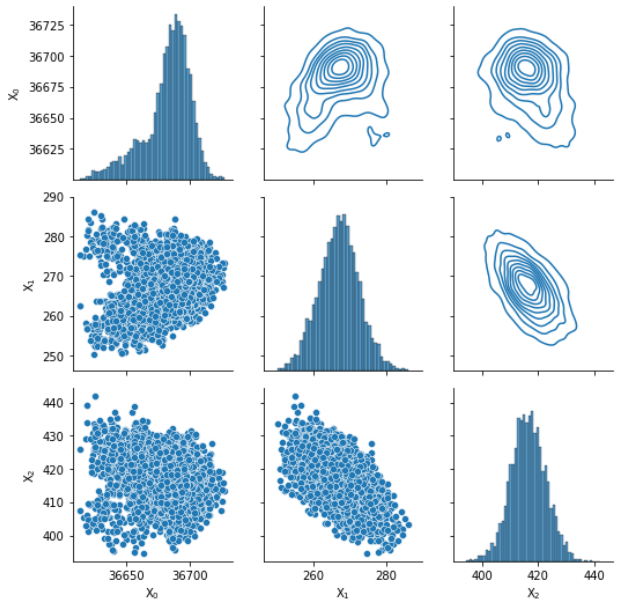

Figure 10: Posterior distribution of PCE coefficients in Example II.

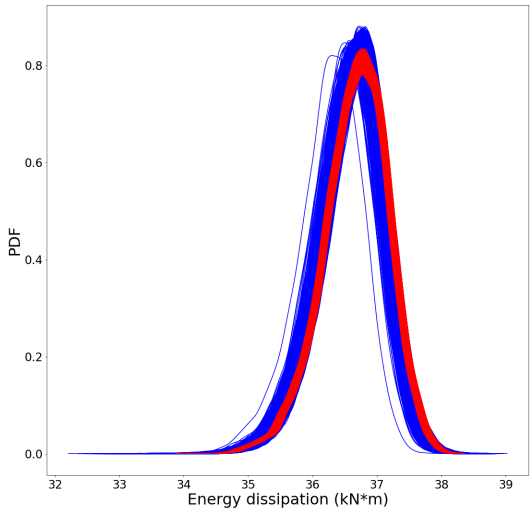

Figure 11: The family of response PDFs computed by posterior PCEs (red) and the family by prior PCEs (blue) in Example II.

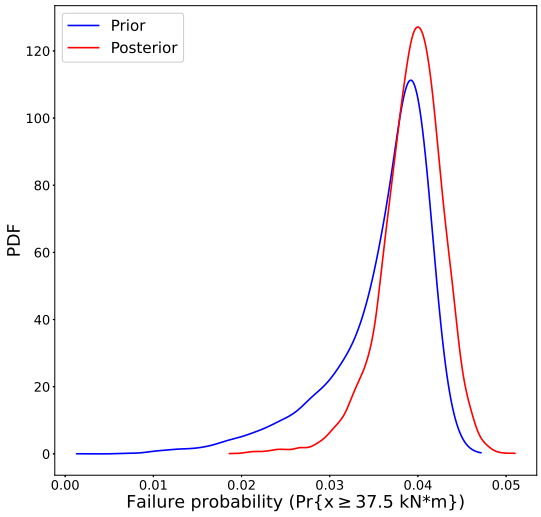

Figure 12: The posterior and prior distributions of the probability of failure in Example II.

coefficients according to Eq. (24) is shown in Fig. 10. A clearly larger scatter is found compared with the prior samples. According to Eq. (26), the two families of response PDFs using prior and posterior PCE models are plotted together in Fig. 11, and the distribution of the probability of failure (P_f) associated with $X > 37.5$ kN*m is shown in Fig. 12. It can be clearly seen that the posterior family is thinner than the prior family, which means the posterior predictions has smaller scatter than the prior predictions. The posterior distribution of failure probability shifts to the right and is sharper than the prior distribution, thus indicating the observations result in an increase in the overall failure probability and gives higher credibility of the prediction.

8. Concluding Remarks

We have presented a Bayesian parameter calibration approach based on a polynomial chaos model whose prior model is constructed as an EPCE. The epistemic uncertainties associated with model inadequacy and incomplete probabilities are accounted for. The performance of the proposed methodology has been assessed using an analytical and a numerical example. Both cases indicate that data assimiliation yields a smaller scatter in the family of response PDFs, and the distribution of failure probability shifts and has a tighter support better aligned with observed data, as expected, and consistent with observations. The Bayesian inference of coefficients in PCE surrogate model allows dual-level characterizations of the uncertainties in QoI, which enables more informative predictions and decision-making than updating the physical parameters in the physics model. It is worth mentioning that the model evaluations in associated Markov chains are performed by the PCE models, resulting in a streamlined and efficient procedure.

In the original version of EPCE, if the statistical parameters $\boldsymbol{P}$ are estimated according to the MLE arguments, then their asymptotic distribution will be Gaussian. However, in the small data case, the distribution of $\boldsymbol{P}$ will generally depend on the dataset. One could replace Eq. (6) with a higher-order PCE to account for more general form of the density function. This will slightly complicate the evaluation of sensitivities with respect to the epistemic variable would be complicated to take. In the present work, the representation of the error associated with the model of $\boldsymbol{P}$ by a chaos expansion of QoI in Eq. (16) can not only account for more general forms of the density function, but can also preserve the convenience to take sensitivities as a straightforward post-processing of the EPCE.

Acknowledgements

Support for this research was provided by the US National Science Foundation under award number 1661052 and from the US Department of Energy SciDac FASTMATH Institute.

References

[1] A. Der Kiureghian, O. Ditlevsen, Aleatory or epistemic? does it matter?, Structural safety 31 (2) (2009) 105–112.
[2] R. G. Ghanem, P. D. Spanos, Stochastic finite elements: a spectral approach, Dover, 2003.
[3] J. Li, J. Chen, Stochastic dynamics of structures, John Wiley & Sons, 2009.
[4] C. Soize, Uncertainty quantification, Springer, 2017.
[5] R. Ghanem, D. Higdon, H. Owhadi, Handbook of uncertainty quantification, Vol. 6, Springer, 2017.
[6] D. Straub, I. Papaioannou, Bayesian updating with structural reliability methods, Journal of Engineering Mechanics 141 (3) (2015) 04014134.
[7] M. Beer, Y. Zhang, S. T. Quek, K. K. Phoon, Reliability analysis with scarce information: Comparing alternative approaches in a geotechnical engineering context, Structural Safety 41 (2013) 1–10.
[8] A. L. Rechenmacher, Z. Medina-Cetina, Calibration of soil constitutive models with spatially varying parameters, Journal of Geotechnical and Geoenvironmental Engineering 133 (12) (2007) 1567–1576.
[9] D. Straub, A. Der Kiureghian, Bayesian network enhanced with structural reliability methods: methodology, Journal of engineering mechanics 136 (10) (2010) 1248–1258.
[10] M. C. Kennedy, A. O'Hagan, Bayesian calibration of computer models, Journal of the Royal Statistical Society: Series B (Statistical Methodology) 63 (3) (2001) 425–464.
[11] C. Soize, Stochastic modeling of uncertainties in computational structural dynamics—recent theoretical advances, Journal of Sound and Vibration 332 (10) (2013) 2379–2395.

[12] R. E. Morrison, T. A. Oliver, R. D. Moser, Representing model inadequacy: A stochastic operator approach, SIAM/ASA Journal on Uncertainty Quantification 6 (2) (2018) 457–496.
[13] K. Sargsyan, X. Huan, H. N. Najm, Embedded model error representation for bayesian model calibration, International Journal for Uncertainty Quantification 9 (4).
[14] K. Sargsyan, H. Najm, R. Ghanem, On the statistical calibration of physical models, International Journal of Chemical Kinetics 47 (4) (2015) 246–276.
[15] M. D. Spiridonakos, E. N. Chatzi, Metamodeling of dynamic nonlinear structural systems through polynomial chaos narx models, Computers & Structures 157 (2015) 99–113.
[16] Y. M. Marzouk, H. N. Najm, L. A. Rahn, Stochastic spectral methods for efficient bayesian solution of inverse problems, Journal of Computational Physics 224 (2) (2007) 560–586.
[17] M. Tootkaboni, L. Graham-Brady, A multi-scale spectral stochastic method for homogenization of multi-phase periodic composites with random material properties, International journal for numerical methods in engineering 83 (1) (2010) 59–90.
[18] K. E. Willcox, O. Ghattas, P. Heimbach, The imperative of physics-based modeling and inverse theory in computational science, Nature Computational Science 1 (3) (2021) 166–168.
[19] M. Beer, P. D. Spanos, A neural network approach for simulating stationary stochastic processes, Structural Engineering and Mechanics, An Int'l Journal 32 (1) (2009) 71–94.
[20] W. Liu, Z. Lai, K. Bacsa, E. Chatzi, Physics-guided deep markov models for learning nonlinear dynamical systems with uncertainty, Mechanical Systems and Signal Processing 178 (2022) 109276.
[21] M. Tootkaboni, L. Graham-Brady, B. W. Schafer, Geometrically non-linear behavior of structural systems with random material property: An asymptotic spectral stochastic approach, Computer Methods in Applied Mechanics and Engineering 198 (37-40) (2009) 3173–3185.
[22] M. Beer, S. Ferson, V. Kreinovich, Imprecise probabilities in engineering analyses, Mechanical systems and signal processing 37 (1-2) (2013) 4–29.
[23] E. Hofer, M. Kloos, B. Krzykacz-Hausmann, J. Peschke, M. Woltereck, An approximate epistemic uncertainty analysis approach in the presence of epistemic and aleatory uncertainties, Reliability Engineering & System Safety 77 (3) (2002) 229–238.
[24] J. Helton, J. Johnson, W. Oberkampf, C. B. Storlie, A sampling-based computational strategy for the representation of epistemic uncertainty in model predictions with evidence theory, Computer Methods in Applied Mechanics and Engineering 196 (37-40) (2007) 3980–3998.
[25] S. Yin, D. Yu, Z. Luo, B. Xia, An arbitrary polynomial chaos expansion approach for response analysis of acoustic systems with epistemic uncertainty, Computer Methods in Applied Mechanics and Engineering 332 (2018) 280–302.
[26] B. Möller, M. Beer, Fuzzy randomness: uncertainty in civil engineering and computational mechanics, Springer Science & Business Media, 2004.
[27] C. Wang, H. G. Matthies, M. Xu, Y. Li, Dual interval-and-fuzzy analysis method for temperature prediction with hybrid epistemic uncertainties via polynomial chaos expansion, Computer Methods in Applied Mechanics and Engineering 336 (2018) 171–186.
[28] M. S. Eldred, L. P. Swiler, G. Tang, Mixed aleatory-epistemic uncertainty quantification with stochastic expansions and optimization-based interval estimation, Reliability Engineering & System Safety 96 (9) (2011) 1092–1113.
[29] R. Ghanem, P. D. Spanos, Polynomial chaos in stochastic finite elements, Journal of Applied Mechanics 57 (1) (1990) 197–202.
[30] R. Ghanem, Ingredients for a general purpose stochastic finite elements implementation, Computational Methods in Applied Mechanics and Engineering 168 (1-4) (1999) 19–34.
[31] Y. M. Marzouk, H. N. Najm, Dimensionality reduction and polynomial chaos acceleration of bayesian inference in inverse problems, Journal of Computational Physics 228 (6) (2009) 1862–1902.
[32] A. Sarkar, R. Ghanem, Mid-frequency structural dynamics with parameter uncertainty, Computer Methods in Applied Mechanics and Engineering 191 (47-48) (2002) 5499–5513.
[33] R. Ghanem, A. Doostan, On the construction and analysis of stochastic predictive models: Characterization and propagation of the errors associated with limited data, Journal of Computational Physics 217 (1) (2006) 63–81.
[34] S. Das, R. Ghanem, J. Spall, Asymptotic sampling distribution for polynomial chaos representation of data : A maximum-entropy and fisher information approach, SIAM Journal on Scientific Computing 30 (5) (2008) 2207–2234.
[35] R. G. Ghanem, A. Doostan, J. Red-Horse, A probabilistic construction of model validation, Computer Methods in Applied Mechanics and Engineering 197 (29-32) (2008) 2585–2595.
[36] M. Arnst, R. Ghanem, C. Soize, Identification of bayesian posteriors for coefficients of chaos expansions, Journal of Computational Physics 229 (9) (2010) 3134–3154.
[37] Z. Wang, R. Ghanem, An extended polynomial chaos expansion for pdf characterization and variation with aleatory and epistemic uncertainties, Computer Methods in Applied Mechanics and Engineering 382 (2021) 113854.
[38] Z. Wang, R. Ghanem, A functional global sensitivity measure and efficient reliability sensitivity analysis with respect to statistical parameters, Computer Methods in Applied Mechanics and Engineering 402 (2022) 115175.
[39] Z. Wang, P. Hawi, S. Masri, V. Aitharaju, R. Ghanem, Stochastic multiscale modeling for quantifying statistical and model errors with application to composite materials, Reliability Engineering & System Safety 235 (2023) 109213.
[40] Z. Wang, R. Ghanem, Stochastic framework for optimal control of planetary reentry trajectories under multilevel uncertainties, AIAA Journal (2023) 1–12.
[41] Z. Wang, R. Ghanem, Stochastic sensitivities across scales and physics, EMI 2019.
[42] E. Jacquelin, M. I. Friswell, S. Adhikari, O. Dessombz, J.-J. Sinou, Polynomial chaos expansion with random and fuzzy

variables, Mechanical Systems and Signal Processing 75 (2016) 41–56.
[43] B. W. Silverman, Density estimation for statistics and data analysis, Vol. 26, CRC press, 1986.
[44] B. R. Ellingwood, K. Kinali, Quantifying and communicating uncertainty in seismic risk assessment, Structural Safety 31 (2) (2009) 179–187.
[45] Z. Wang, Z. Gao, Y. Wang, Y. Cao, G. Wang, B. Liu, Z. Wang, A new dynamic testing method for elastic, shear modulus and poisson's ratio of concrete, Construction and Building Materials 100 (2015) 129–135.
[46] P. Gardoni, A. Der Kiureghian, K. M. Mosalam, Probabilistic capacity models and fragility estimates for reinforced concrete columns based on experimental observations, Journal of Engineering Mechanics 128 (10) (2002) 1024–1038.
[47] D. Feng, J. Li, Stochastic nonlinear behavior of reinforced concrete frames. ii: Numerical simulation, Journal of Structural Engineering 142 (3) (2016) 04015163.
[48] D.-C. Feng, S.-C. Xie, J. Xu, K. Qian, Robustness quantification of reinforced concrete structures subjected to progressive collapse via the probability density evolution method, Engineering Structures 202 (2020) 109877.
[49] J. H. Thomsen IV, J. W. Wallace, Displacement-based design of slender reinforced concrete structural walls—experimental verification, Journal of structural engineering 130 (4) (2004) 618–630.
[50] A. C. 318, Building code requirements for structural concrete (aci 318-19): An aci standard: Commentary on building code requirements for structural concrete (aci 318r-19), Tech. rep., American Concrete Institute (2019).
[51] S. Hibbitt, Karlsson, Abaqus/standard user's manual, Tech. rep., Hibbitt, Karlsson & Sorensen (2001).
[52] D.-C. Feng, X.-D. Ren, J. Li, Cyclic behavior modeling of reinforced concrete shear walls based on softened damage-plasticity model, Engineering Structures 166 (2018) 363–375.